Experimental characterization of friction properties of materials for innovative beam-to-column dissipative connection for low-damage RC structures

Available online at www.sciencedirect.com

ScienceDirect

Procedia Structural Integrity 44 (2023) 1909–1916

Structural Integrity Procedia

www.elsevier.com/locate/procedia

XIX ANIDIS Conference, Seismic Engineering in Italy

Experimental characterization of friction properties of materials for innovative beam-to-column dissipative connection for low-damage RC structures

Salvatore Pagnotta[a,*], Alessia Monaco[b], Piero Colajanni[a], Lidia La Mendola[a]

[a] *Department of Engineering, Unversity of Palermo, Viale delle Scienze, Ed. 8, Palermo 90128, Italy*
[b] *Department of Architecture and Design, Politecnico di Torino, Viale Mattioli 39, Torino 10125, Italy*

Abstract

Low-damage design of structures in seismic-prone areas is becoming an efficient strategy to obtain "earthquake-proof" buildings, i.e. buildings that, even in the case of severe seismic actions, experience a low or negligible amount of damage. Besides the safeguard of human lives, this design strategy aims also to limit the downtime of buildings, which represents a significant source of economic loss, and to ensure an immediate occupancy in the aftermath of an earthquake. In this context, focusing on moment-resisting frames (MRFs), several solutions have been developed for the beam-to-column connections (BCCs) of steel and precast/prestressed concrete structures, but very few for cast-in-situ reinforced concrete (RC) structures. This paper focuses on a recently-proposed friction-based BCC for MRFs made with hybrid steel-trussed concrete beams (HSTCBs). The latter are made by a spatial lattice built using V-shaped rebars and a steel bottom plate, which eases the introduction of a friction dissipative device. HSTCBs are usually characterized by a small effective depth, which leads to a large amount of longitudinal rebars. The latter, together with a small-sized beam-column joint, make it potentially subjected to severe damage, which reduces its dissipative capacity. The shear force acting on the joint can be reduced by endowing the BCC with a friction device, with the aim of increasing the lever arm of the bending moment transferred between beam and joint, preventing the latter from damage. To evaluate the mechanical performance of the above connection, two experimental programs have been carried out at the Structures Laboratory of the University of Palermo. The first one focused on the characterization of the friction properties of two different materials (thermal sprayed aluminum and brass), by means of a linear dissipative device subjected to cyclic load. The second one tested a beam-to-column subassembly endowed with the recently-proposed connection in which the dissipative device was made with the best performing friction material tested before. The results of the cyclic tests are presented and commented, showing the promising performance of such connection in providing a low-damage behavior and a satisfactory dissipative capacity.

Keywords: Friction dampers; Hybrid steel-trussed concrete beams; RC joints; Experimental test; Earthquake design

10.1016/j.prostr.2023.01.244

1. Introduction

A new design strategy for structures in earthquake-prone areas has been developed by practitioners and researchers during the last twenty years aimed at achieving earthquake-proof buildings, i.e. buildings which experience a negligible level of damage even if subjected to destructive seismic actions. Focusing on the solutions proposed for moment-resisting frame (MRF) structures, several devices were developed for steel structures (e.g. Khoo et al. 2012, Latour et al. 2015, Latour et al. 2018, Ramhormozian et al. 2018, Yang and Popov 1995), but very few devices were specifically proposed for cast-in-situ reinforced concrete. Recently, Colajanni et al. (2020a, 2021a) proposed a friction-based beam-to-column connection (BCC) for MRFs made with hybrid steel-trussed concrete beams (HSTCBs). The latter are made by a spatial lattice built using V-shaped rebars and a steel bottom plate, which eases the introduction of a friction dissipative device. HSTCBs are usually characterized by a small effective depth, which leads to a large amount of longitudinal rebars. The latter, together with a small-sized beam-column joint, make it potentially subjected to severe damage, which reduces its dissipative capacity. The shear force acting on the joint can be reduced by endowing the BCC with a friction device, with the aim of increasing the lever arm of the bending moment transferred between beam and joint, preventing the latter from damage. The use of this connection was proved numerically to be effective in reducing the damage undergone by RC frames during a severe earthquake (Colajanni et al. 2021b). The present research aims to experimentally evaluate the mechanical response of a beam-column subassembly endowed with the proposed friction dissipative connection. A specimen scale 1:1 is made and subjected to a reversed cyclic loading. To evaluate the friction properties of the materials used in the dissipative connection, a linear friction dissipative device is tested using a loading protocol consistent with the suggestions of EN15129:2018. Two materials are investigated, selected among the most performing ones tested over the last two decades and reported in the literature: thermal sprayed aluminum and brass. The evaluation of the friction coefficient over time is obtained monitoring the preload acting on the bolts belonging to the sliding bolted connection.

2. Beam-to-column connection for cast-in-situ RC MRFs

The proposed beam-to-column connection is suitable for columns and beams with any geometrical or mechanical characteristics. A prototype of the connection was designed on the basis of the beam-column subassembly described in Colajanni et al. (2016), whose main characteristics are: cross-sectional dimensions of beam = 300 x 250 mm^2, cross-sectional dimensions of column = 400 x 300 mm^2, longitudinal rebars of beam = 4ϕ24 (top) + 2ϕ24 (bottom), longitudinal rebars of column = 10ϕ20, transverse reinforcement of beam = ϕ8/6 cm, transverse reinforcement of column = ϕ8/11 cm. The truss of the HSTC beam is endowed with a 5 mm-thick steel bottom plate and a truss made with 2 inclined rebars ϕ12 arranged at 30 cm of spacing. The hogging and sagging moment strength of the beam are equal to 165 kNm and 90 kNm, respectively, while the shear strength can be calculated using the analytical model proposed in Colajanni et al. (2020b), which develops that proposed in Colajanni et al. (2015), and it is equal to 350 kN. The main elements constituting the proposed connection are described below (Fig. 1 (a)): on the bottom side of the steel plate of the HSTC beam it is inserted a friction dissipative device, which is made with two steel angles (blue) and a central plate (red) with curved slotted holes. The plates are clamped together through high strength preloaded bolts; on the top side of the HSTC beam, a top horizontal plate (green) is added, which is connected on the bottom side with the vertical central plate, and on the top side with the longitudinal rebars of the HSTC beam; between top horizontal plate and column, there is a T stub (cyan), which ensures the connection between the beam (through an ordinary friction bolted connection) and the column (through preloaded threaded bars); the connection between the concrete block of the HSTC beam, the steel truss and the plates constituting the dissipative device is ensured by perfobond connectors made on the embedded part of the vertical central plate and studs (yellow) added between the top horizontal plate and the bottom steel plate. The proposed connection is designed in order to rotate around a center of rotation which is supposed to form close to the base section of the T stub. The curved slotted holes, through which the bolts belonging to the dissipative device are supposed to move, are defined on the basis of the above center of rotation, designing the axial length, the cross-sectional width and the radius with the aim of avoiding any contact between the bolts and the central plate up to the design rotation of the connection. By doing so, once the connection begins to slide, no other contribution arises during the sliding phase, keeping the moment capacity provided by the connection almost constant up to the contact of bolt shanks with the end section of the curved slotted holes.

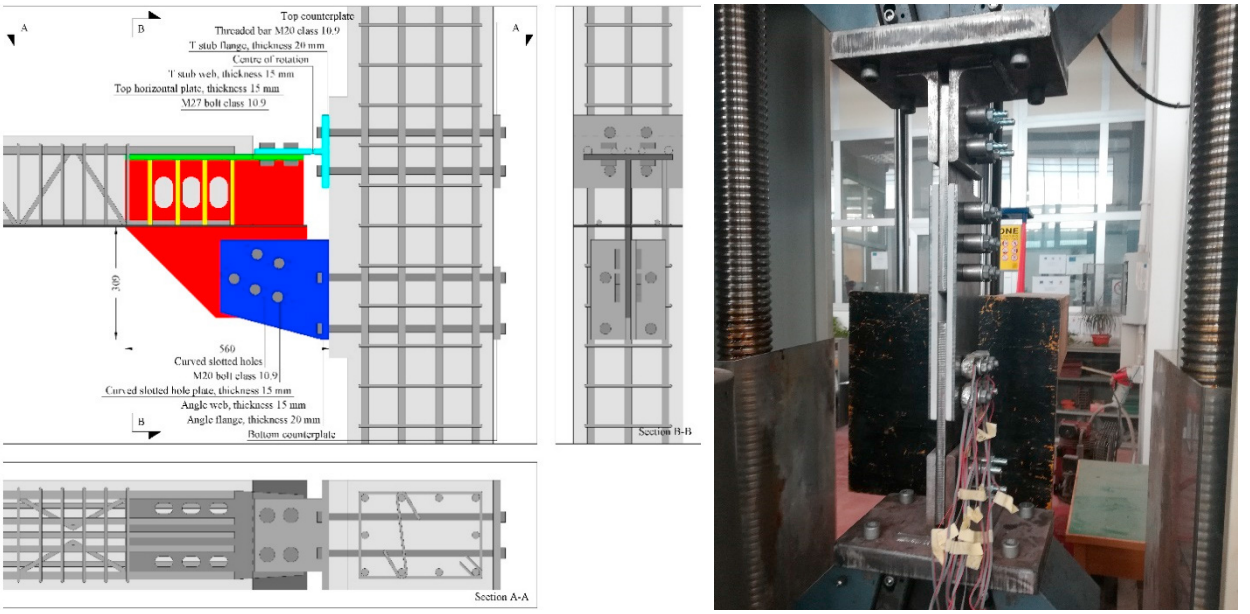

Fig. 1. (a) beam-column joint endowed with friction connection; (b) test setup of the linear friction dissipative device.

3. Experimental test on the linear friction dissipative device

The linear friction device used to assess the friction properties of the two friction pads investigated is similar to that tested by Latour et al. (2014). In detail, the device is constituted by two steel plates, one with standard clearance hole and the other one with slotted holes, connected by means of a double cover butt joint having four preloaded bolts M12 class 10.9 on the sliding side and six on the fixed side. Between the two steel plates and the cover plates are inserted two friction shims made with thermal sprayed aluminum or brass. The central plates are connected by means of bolted shear connections to four steel angles welded to 35 mm-thick steel plates bolted to the Universal Testing Machine (UTM) (Fig. 1 (b)). The design of the linear friction device is carried out according to EN1993-1-1. With the aim of keeping the preloading force acting on the bolts of the friction device as constant as possible, three disc springs arranged in series are added to each bolt. Two tests are carried out for each group of friction shims, with the aim of investigating the friction coefficient values of the already-used material. The preload applied on each bolt is 24 kN, which is equal to 40% of the code-consistent bolt preload (60 kN). The loading protocol is developed starting from the requirements of the EN15129:2018. Assuming a maximum displacement of the device of 30 mm, the loading protocol is constituted by 5 cycles at 25% of the maximum displacement (± 7.5 mm), 5 cycles at 50% of the maximum displacement (± 15 mm), and 10 cycles at 100% of the maximum displacement (± 30 mm).

The test 1 was carried out on brand new plates coated with thermal sprayed aluminum, which showed a significant superficial roughness due to the production technique. The force-displacement curve of the first test is shown in Fig. 2 (a). Overall, it can be seen that the curve is characterized by sections in which the sliding force is constant and sections where it shows sudden variations. The latter phenomenon is called "*stick and slip*", namely the sliding of the device is not continuous (even if the test is carried out in displacement control mode) and the central plate slides unevenly. Once the sliding force is achieved, the plate starts to slide, which leads to a reduction on the force acting on it due to due difference between static and dynamic friction coefficient, and the plate stops once again. At this point the load increases until the sliding force is achieved again. The device began sliding at 140 kN, and then the force significantly reduced to 90 kN during the first loading cycle. In the following ones, the sliding force tends to decrease until it is in the range of 70 kN in the last ± 30 mm amplitude cycles. The difference between the initial and final sliding force is about 50%. With regard to the friction coefficient, whose trend over time is shown in Fig. 3 (a), it is possible to note an uneven behavior. In fact, in the first part of the test, the friction coefficient increased from 0.62 to 0.75. Then, there is a reduction up to a value of 0.57 at the end of the test. The preload force acting on the bolts during

the test is shown in Fig. 4 (a). In general, there is a decreasing trend over time with a significant reduction from the initial preload. In detail, in the very early stages of the test, that is, at the moment when the slotted center plate starts to slide, there is a sudden loss of preload on all four bolts. This decrease is due to a settling of the bolt-disc spring-load cell assembly due to the movement of the plates, which resulted in significant bolt loosening that was not compensated by the disc springs. As a result of this initial loss of preload, there is an asymptotic trend in the preload acting on the bolts to an average final value of about 15.5 kN, 35% lower than the initial value of 24 kN. As a result of the above analysis of the results, it can be stated that the change in sliding force that is recorded on the dissipative device during the test is mainly due to the change in preload acting on the bolts, the initial and final differences of the two quantities being similar in percentage terms.

Starting from the final configuration of test 1, thus without disassembling or replacing the bolts, test 2 was carried out after applying the design preload of 24 kN to the bolts of the sliding friction connection. The force-displacement curve of test 2 is shown in Fig. 2 (b). Unlike what was seen before in test 1, there are no longer any significant changes in the sliding force in the initial phase. The initial sliding force is about 110 kN, while the final sliding force is 95 kN, a difference of about 15%, which is much less than previously recorded. Significant differences from the previous test can also be found for the trend of the friction coefficient over time (Fig. 3 (b)). In fact, it can be seen that the value remains approximately constant throughout the test, with small fluctuations and a slight decrease in the final part of the test itself. The initial value is 0.6, while the final value is 0.57, a difference of about 5%. This result highlights the ability of thermal sprayed aluminum to provide remarkable performance following a far greater number of cycles than required by EN15129. Once the outermost surface roughness flattens out and the surfaces tend to smooth out, the wear rate of thermal sprayed aluminum stabilizes as the number of cycles increases, providing a virtually unchanged friction coefficient during the test. Regarding the trend of preload on the bolts over time (Fig. 4 (b)), significant differences from Test 1 can be seen. In fact, the significant loss of preload recorded at the beginning of the test was not repeated in Test 2, although a loss on the order of 5% of the initial preload occurs in the initial stages when the slotted plate starts to slide. During the rest of the test, the average preload on the bolts tends to decrease asymptotically to a final average value of about 21.5 kN, which is almost 10% less than the initial value.

Test 3 was carried out using plates made of brass as friction shims. Unlike aluminum, brass had very low surface roughness to the touch. The phenomenon of "stick and slip" is even more pronounced in the force-displacement curve shown in Fig. 6 (a), with significant fluctuations in the slip force during the application of displacement. In general, the slip force tends to increase as the number of cycles performed and the displacement achieved increases. The first cycle is characterized by a sliding force in the range of 35 kN, which reaches 62 kN at the end of the first five cycles with amplitude ± 7.5 mm. At the end of the test the sliding force reached values of about 85 kN, with a difference from the initial value of more than 140%. The explanation for the result shown in Fig. 5 (a) can be found by looking at the trend of the friction coefficient over time shown in Fig. 6 (a). The friction coefficient increases gradually, rising from 0.25 to a value of about 0.43 from the second half of the test onward. This increase is due to surface wear of the brass, which has led to roughening of the surfaces resulting in an increase in the friction coefficient. Regarding the preload acting on the bolts (Fig. 7 (a)), unlike what was observed previously for test 1, there is no substantial loss of preload at the beginning of the test. In addition, the average preload value of the bolts remained practically constant throughout the test, albeit with significant fluctuations in preload force. Based on this result, it is possible to say that the variations in sliding force are mostly due to the variations in friction coefficient between the contact plates.

Also in the case of the brass plates, a second test was performed from the final configuration of test 3, again applying the design preload of 24 kN to the bolts of the sliding friction connection. The force-displacement curve of test 4 (Fig. 5 (b)) shows a significantly different trend from what was previously observed. In fact, the hysteresis cycles show a virtually constant sliding force over time, with initial value of 85 kN and final value of 78 kN (8% difference). The stability of the sliding force is a direct consequence of the stability of the friction coefficient, as can be seen in Fig. 6 (b). In fact, the value of friction coefficient expressed by the two contact plates, which is about 0.45, remains practically constant throughout the test. In analogy to what was seen previously, the trend of the preload acting on the bolts (Fig. 7 (b)), although characterized by considerable fluctuations in the values during sliding, shows an average value that is substantially constant and equal to 24 kN. From the results obtained, it is possible to state that, even in the case of brass plates, the results obtained during a second cyclic test are considerably better than those obtained with the first, since, during the first test, the surfaces of the plates change their roughness characteristics until they stabilize and remain constant during the second test.

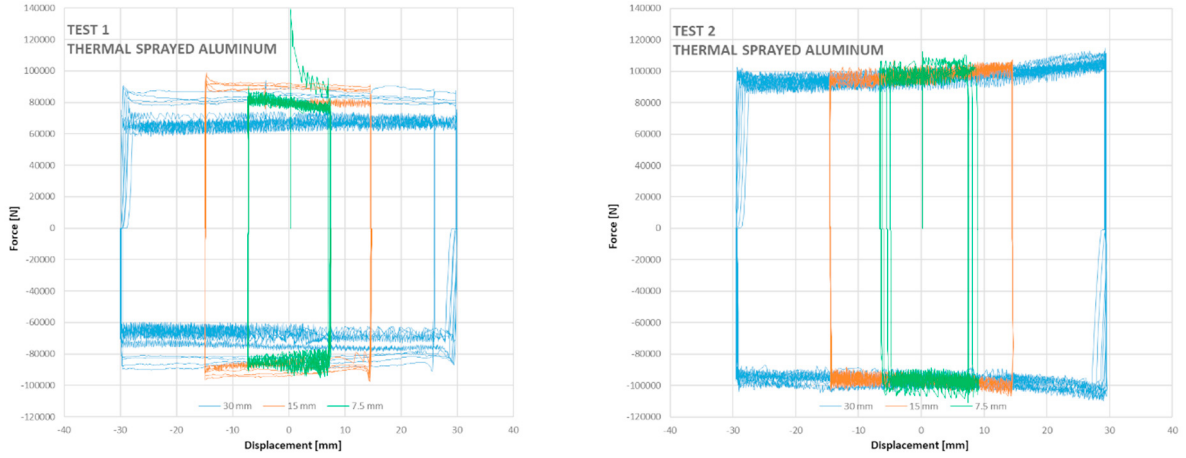

Fig. 2. (a) force-displacement curve of test 1; (b) force-displacement curve of test 2.

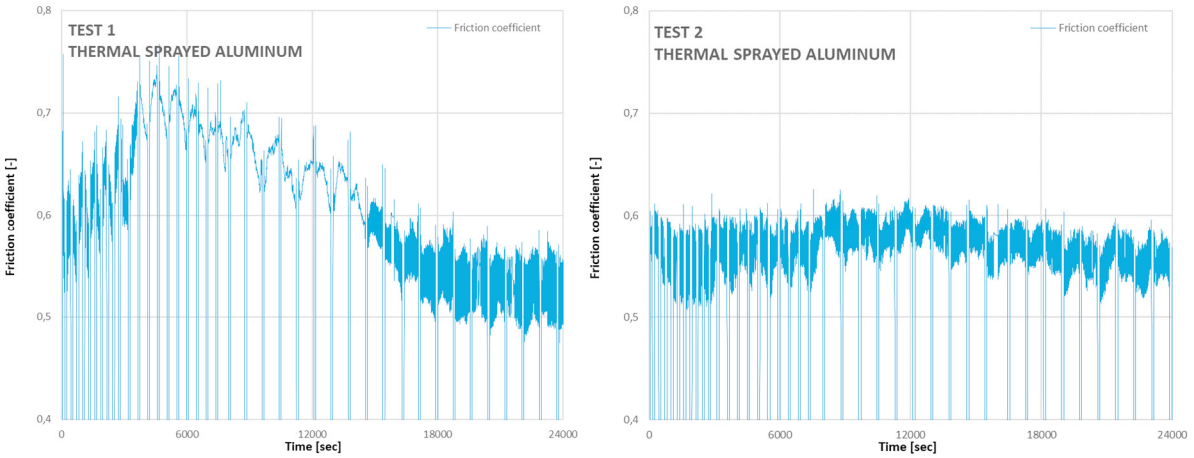

Fig. 3. (a) friction coefficient trend during test 1; (b) friction coefficient trend during test 2.

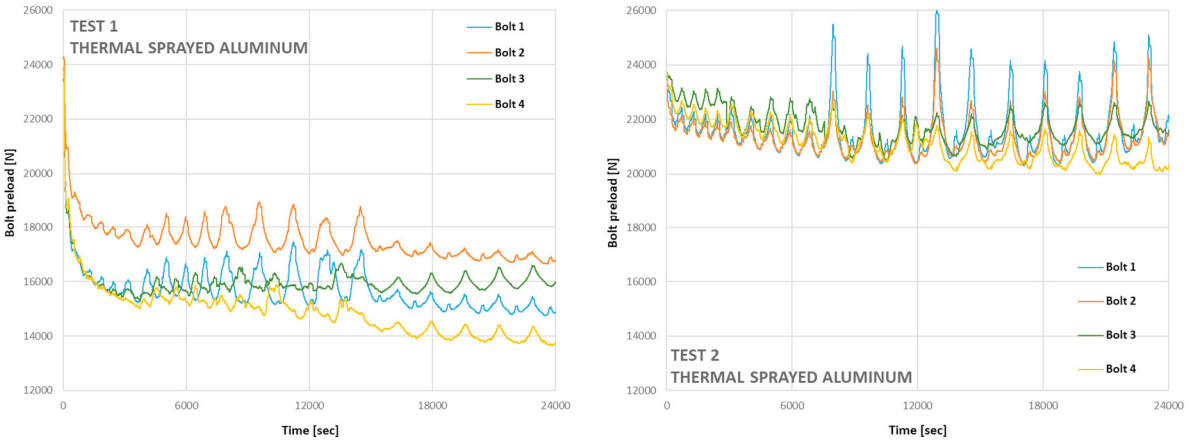

Fig. 4. (a) trend of preload acting on bolts during test 1; (b) trend of preload acting on bolts during test 2.

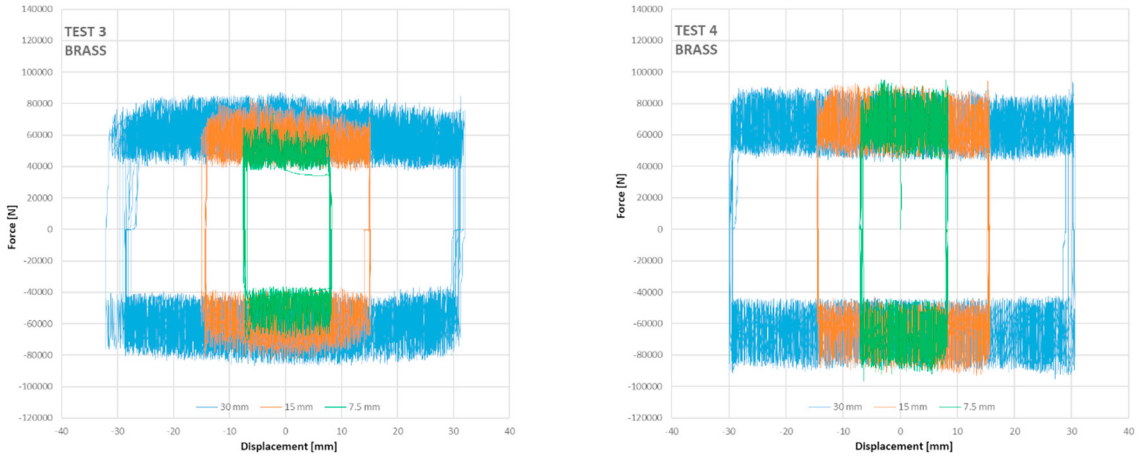

Fig. 5. (a) force-displacement curve of test 3; (b) force-displacement curve of test 4.

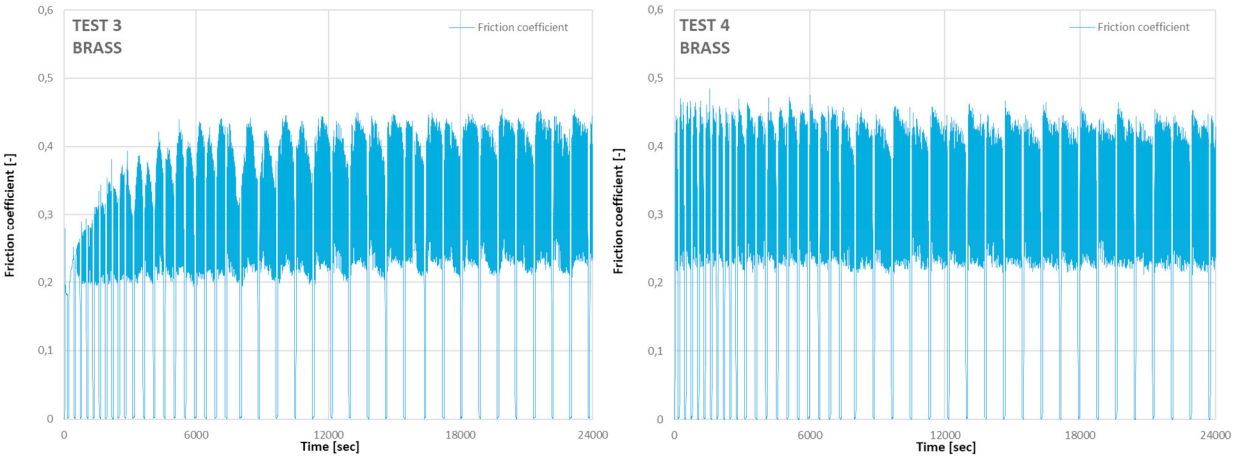

Fig. 6. (a) friction coefficient trend during test 3; (b) friction coefficient trend during test 4.

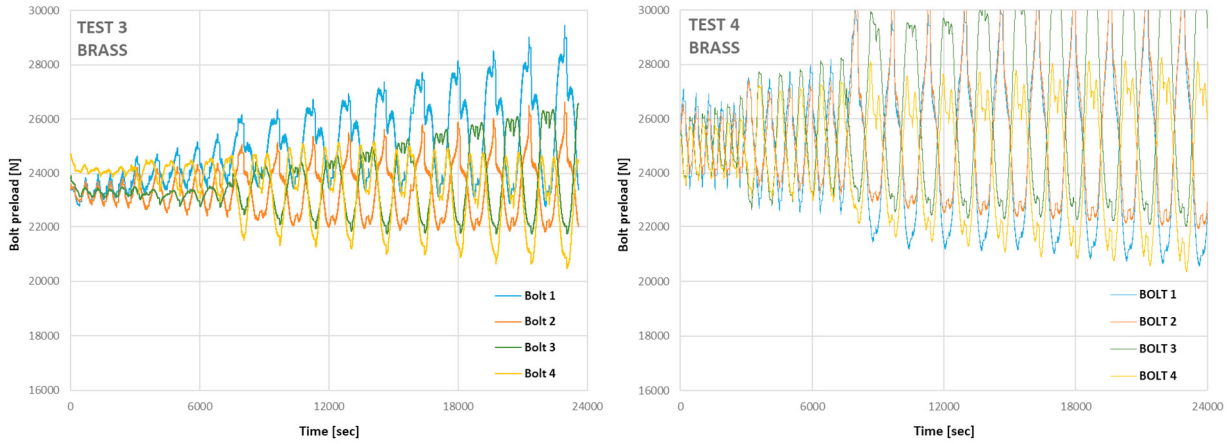

Fig. 7. (a) trend of preload acting on bolts during test 3; (b) trend of preload acting on bolts during test 4.

4. Experimental test on the beam-column joint endowed with friction connection

On the basis of the results reported above, it can be stated that the best-performing friction material is the thermal sprayed aluminum, since it provided the highest friction coefficient with a remarkable stability, only once the surface is already worn by a preliminary test. Assuming a friction coefficient of 0.6, the design of a specimen of the beam-column joint described in Section 2 were carried out. The specimen is constituted by an external beam-column joint (Fig. 8 (a)), in which the column is a HEB300 steel profile 3.3 m long and a HSTC beam 1.55 m long. The T stub was made from a HEB300 profile in order to simplify the construction process. The connection between T stub and column was made with four M24 bolts class 10.9, while that between T stub and HSTCB was made with eight M20 bolts class 10.9. To reduce the components constituting the dissipative device, the friction pads were not considered, and the coating of thermal sprayed aluminum was made on the steel angles (Fig. 8 (b)). The connection between steel angles and vertical central plate was constituted by five M20 bolts class 10.9, while that between steel angles and column was made with four M24 bolts class 10.9. An axial load of 100 kN was applied on the column to simulate the effect of dead load. The displacement-controlled test was carried out by applying on the beam, at a distance from the center of rotation of l = 1.31 m, a displacement history defined on the basis of the suggestions of ACI 374.2R-13 (2013). The amplitudes of the cycles were determined by using the yield rotation (equal to 2.5 mrad) multiplied by an increasing coefficient. Five amplitudes were considered, having maximum displacement of ± 2 mm, ± 5 mm, ± 10 mm, ± 20 mm and ± 40 mm. Two cycles were carried out for each amplitude. The bolts of the friction device were torqued to achieve a preload of 17 kN, so that the yielding moment of the connection can be calculated as $M_y = \mu\, n_b\, n_s\, F_{pc}\, z$ = 38 kNm, where μ is the friction coefficient, n_b the number of bolts (5), n_s the number of surfaces (2), F_{pc} the preload on each bolt (17 kN), and z the internal lever arm of the connection. The expected sliding force, equal to 29 kN, is obtained dividing M_y by l. The force-displacement curve obtained during the cyclic test is shown in Fig. 9. Generally speaking, the preliminary results showed that the beam-column joint provided hysteresis loops which are wide and stable, and no damage nor cracking were observed on the specimen. The hysteresis loops are characterized by a higher value of sliding force in the case of sagging moment and a lower value in the case of hogging moment. The sliding force tended to reduce during the test, due to the same phenomena affecting the behavior of the linear dissipative device, namely loss of preload force acting on the bolts and wearing of the surfaces in contact. Similarly to the results of test 1 on the linear dissipative device, the curve is characterized by sections in which the device slid constantly and sections where it showed the “stick and slip” phenomenon, although less pronounced. The variation of force due to the latter phenomenon, being not significant, did not affect noticeably the overall response of the connection, differently from what was seen during the tests on the linear dissipative device.

Fig. 8. (a) specimen of the innovative beam-column joint endowed with friction dissipative device; (b) detail of the friction dissipative device.

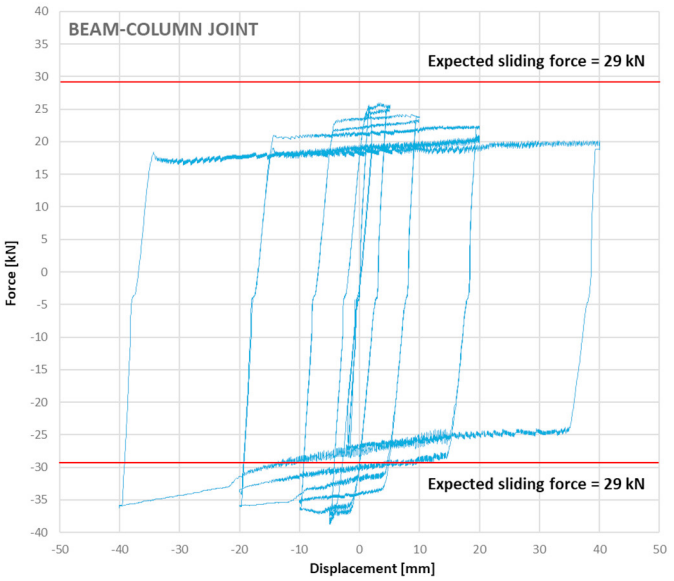

Fig. 9. Force-displacement curve of the beam-column joint endowed with the friction dissipative device.

Acknowledgements

The authors want to thank the company SICILFERRO TORRENOVESE s.r.l. (Italy) for the economic support.

References

ACI-374.2-R-13, 2013. Guide for testing reinforced concrete structural elements under slowly applied simulated seismic loads. Reported by ACI committee 374, American Concrete Institute: Farmington Hills, MI, USA.

Colajanni, P., La Mendola, L., Monaco, A., Pagnotta, S., 2020a. Dissipative connections of rc frames with prefabricated steel-trussed-concrete beams. Ingegneria Sismica 37, 51-63, http://ingegneriasismica.org/product/5-2020-1-dissipative-connections-of-rc-frames-with-prefabricated-steel-trussed-concrete-beams.

Colajanni, P., La Mendola, L., Monaco, A., Spinella, N., 2016. Cyclic behavior of composite truss beam-to-RC column joints in MRFs. Key Engineering Materials 711, 681-689. https://doi.org/10.4028/www.scientific.net/KEM.711.681.

Colajanni, P., Pagnotta, S., Recupero, A., Spinella, N., 2020b. Shear resistance analytical evaluation for RC beams with transverse reinforcement with two different inclinations. Materials and Structures, 53, 18. https://doi.org/10.1617/s11527-020-1452-8.

Colajanni, P., Recupero, A., Spinella, N., 2015. Shear strength degradation due to flexural ductility demand in circular RC columns. Bulletin of Earthquake Engineering 13, 1795-1807. https://doi.org/10.1007/s10518-014-9691-0.

Colajanni, P., La Mendola, L., Monaco, A., Pagnotta, S., 2021a. Design of RC joints equipped with hybrid trussed beams and friction dampers. Engineering Structures 227, 111442. https://doi.org/10.1016/j.engstruct.2020.111442.

Colajanni, P., La Mendola, L., Monaco, A., Pagnotta, S., 2021b. Seismic performance of earthquake-resilient RC frames made with HSTC beams and friction damper devices. Journal of Earthquake Engineering, in press. https://doi.org/10.1080/13632469.2021.1964652.

EN 1993-1-1 (2005): design of joints - Design of steel structures. CEN

EN 15129 (2018): anti-seismic devices. CEN

Khoo, H. H., Clifton, C., Butterworth, J., MacRae, G., Ferguson, G., 2012. Influence of steel shim hardness on the Sliding Hinge Joint performance. Journal of Constructional Steel Research 72, 119-29. https://doi.org/10.1016/j.jcsr.2011.11.009.

Latour, M., Piluso, V., Rizzano G., 2014. Experimental analysis on friction materials for supplemental damping devices. Construction and Building Materials 65, 159-176. https://doi.org/10.1016/j.conbuildmat.2014.04.092.

Latour, M., Piluso, V., Rizzano, G., 2015. Free from damage beam-to-column joints testing and design of DST connections with friction pads. Engineering Structures 85, 219-233. https://doi.org/10.1016/j.engstruct.2014.12.019.

Latour, M., Piluso, V., Rizzano, G., 2018. Experimental analysis of beam-to-column joints equipped with sprayed aluminium friction dampers. Journal of Constructional Steel Research 146, 33-48. https://doi.org/10.1016/j.jcsr.2018.03.014.

Ramhormozian, S., Clifton, G. C., MacRae, G. A., Khoo, H. H., 2018. The sliding hinge joint: final steps towards an optimum low damage seismic-resistant steel system. Key Engineering Materials 763, 751-60. doi: 10.4028/www.scientific.net/KEM.763.751.

Yang, T. S., Popov, E. P., 1995. Experimental and analytical studies of steel connections and energy dissipators. UCB/EERC-95/13, College of Engineering, University of California, Berkeley, USA.